Available online at www.sciencedirect.com

ScienceDirect

Remote Sensing of Environment 112 (2008) 314–325

Remote Sensing of Environment

www.elsevier.com/locate/rse

Comparison of ground-based and remotely-sensed surface soil moisture estimates over complex terrain during SMEX04

Enrique R. Vivoni [a,*], Mekonnen Gebremichael [a], Christopher J. Watts [b], Rajat Bindlish [c], Thomas J. Jackson [c]

[a] Department of Earth and Environmental Science, New Mexico Institute of Mining and Technology, Socorro, NM 87801, United States
[b] Departamento de Física, Universidad de Sonora, Hermosillo, Sonora, Mexico
[c] USDA-ARS Hydrology & Remote Sensing Lab, Beltsville, MD 20705, United States

Received 30 June 2006; received in revised form 10 October 2006; accepted 21 October 2006

Abstract

Comparisons to ground-based surface soil moisture estimates are necessary to evaluate the capability of remote sensors to determine soil moisture and its spatiotemporal variability. Soil moisture can be especially variable in regions of complex terrain which exhibit large variations in vegetation, soil properties and hydrologic conditions. The objective of this study is to evaluate the spatiotemporal variability of soil moisture in a mountainous basin in northwestern Mexico. Soil moisture estimates from ground sampling over a topographic transect and high resolution retrievals from the Polarimetric Scanning Radiometer are compared during a two week period in August 2004 as part of the Soil Moisture Experiment 2004. Results indicate that the soil moisture estimates exhibit similar variability with mean water content. Statistical analysis, however, reveals clear differences in soil moisture in the basin, in particular for wet periods and high elevations. Despite these differences, the temporal persistence of soil moisture from the estimates agrees well and indicates locations that capture the basin-averaged conditions. Furthermore, the spatiotemporal soil moisture characteristics from the two products are linked to terrain attributes. As a result, a hypsometric technique is shown to improve comparisons between basin-averaged values derived from ground data and remote sensing, as compared to arithmetic averaging. To our knowledge, this study is the first attempt to evaluate PSR/CX retrievals with respect to ground observations over a region of high topographic and vegetation variability using statistical, time-stability and terrain analysis techniques.

Keywords: Soil Moisture Experiment 2004; North American monsoon; Watershed soil moisture variability; Aircraft remote sensing; Topographic control; Semiarid hydrology

1. Introduction

Soil moisture is a key state variable of the land surface and governs important processes such as the rainfall-runoff transformation and the partitioning of latent and sensible heat fluxes (Eltahir, 1998; Entekhabi, 1995). In semiarid areas, low and variable precipitation amounts lead to highly dynamic soil moisture distributions in space and time (Gómez-Plaza et al., 2000; Houser et al., 2000; Martínez-Fernández & Ceballos, 2005). Over mountainous areas in the semiarid southwestern US and northwestern Mexico, soil moisture is thought to influence the dynamics of the North American monsoon (NAM) and its hydrologic response (Gochis et al., 2006; Zhu et al., 2005). Nevertheless, much is unknown about the mechanisms through which soil moisture may affect the monsoon onset, sustenance and demise. A large part of this uncertainty is due to a lack of knowledge on the spatiotemporal patterns of soil moisture in the semiarid region.

Surface soil moisture variability in mountain regions is poorly understood due to the lack of ground observations and high-resolution remotely-sensed imagery. Earlier studies have measured the variability in soil moisture along elevation

* Corresponding author. Department of Earth and Environmental Science, New Mexico Institute of Mining and Technology, 801 Leroy Place, MSEC 244, Socorro, NM 87801, United States. Tel.: +1 505 835 5611; fax: +1 505 835 5634.
E-mail address: vivoni@nmt.edu (E.R. Vivoni).

0034-4257/$ - see front matter © 2007 Elsevier Inc. All rights reserved.
doi:10.1016/j.rse.2006.10.028

gradients (Crave & Gascuel-Odoux, 1997; Famiglietti et al., 1998; Hawley et al., 1983; Mohanty et al., 2000), but have typically been limited to small scales (~100 m) in areas lacking strong elevation differences. As a result, relatively little is currently known about soil moisture variability over large areas characterized by complex topography (i.e., ridges and valleys). Furthermore, terrain features in regions of high relief typically impact the distribution of soil texture and vegetation, which in turn exert controls on soil moisture (e.g., Jacobs et al., 2004; Kim & Barros, 2002; Mohanty & Skaggs, 2001). Understanding soil moisture variability at large scales over mountain areas is essential for adequate evaluation of remotely-sensed estimates for large parts of the Earth.

A promising approach for gaining new understanding of surface soil moisture variability in mountain regions is through combining ground observations and remote sensing. Aircraft and satellite sensors can provide spatially-extensive soil moisture estimates at particular overpass times, while continuous ground observations are useful at small scales. Nevertheless, difficulties exist in regions of complex terrain with dense vegetation (Jackson et al., 2005), pointing to the need for ground-truthing remote sensing data. Differences exist, for example, in sampling period, spatial resolution and estimation method which affect comparisons between ground and remote sensing data. In mountain regions, the topographic signatures observed in soil moisture fields, in particular for periods after rainfall, may be useful for aggregating ground data to remotely-sensed scales using the topographic field (e.g., Grayson et al., 1997; Kim & Barros, 2002).

In this study, our objective is to compare ground-based observations and remotely-sensed estimates of soil moisture to understand spatiotemporal variability in a mountainous catchment. The study was carried out from August 3 to 14, 2004 during the Soil Moisture Experiment 2004 (SMEX04). During the period, soil moisture was estimated from an aircraft-based Polarimetric Scanning Radiometer (PSR/CX) and from sampling along a topographic transect encompassing a mountain watershed. Particular emphasis is placed on the role played by terrain attributes on the soil moisture characteristics. While the estimates are limited in temporal extent, the observations are valuable for improving our understanding of soil moisture variability in the NAM region.

2. Methods

In the following, we describe the study region, the ground and remotely-sensed data sets and the analyses techniques used to investigate the soil moisture distributions. Our experimental plan is based on similar soil moisture field campaigns conducted over large regions for validating remote sensing data (e.g., Cosh et al., 2004; Famiglietti et al., 1999). We adapted the sampling strategy to capture soil moisture variability over various elevation bands in the region.

2.1. Study Region

The 75-km by 50-km study region is located in northern Sonora, Mexico (Fig. 1) in a rural region characterized by mountainous terrain, ephemeral streams and seasonally-green vegetation during the monsoon. Mean annual rainfall ranges from 400 to 500-mm, with 50–70% occurring during the summer period (Comisión Nacional del Agua, 2002). Topography is characterized by a high mean elevation and a large elevation range. Two major ephemeral rivers flow north–south

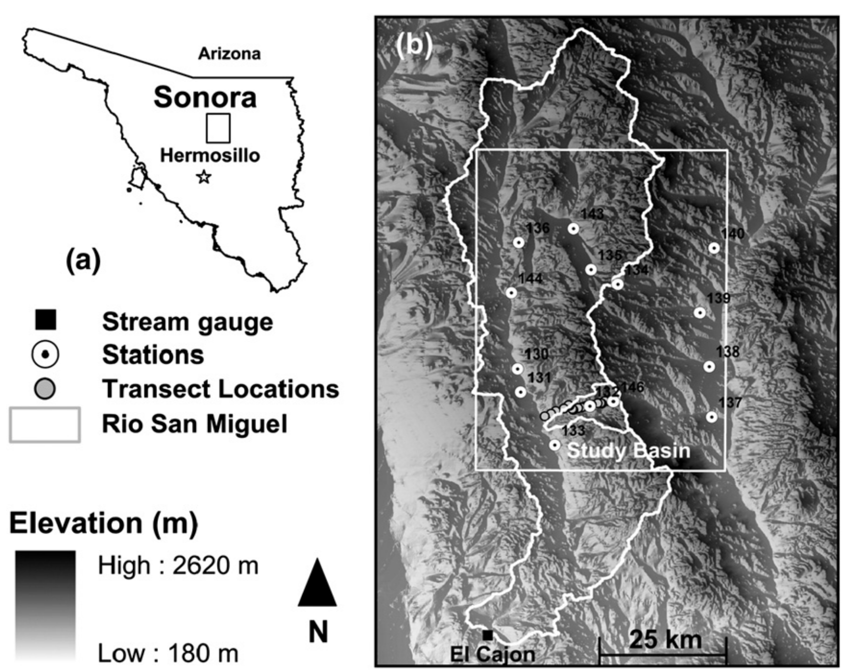

Fig. 1. (a) Regional SMEX04 study area (75-km by 50-km box) in northern Sonora, México. (b) Location of transect sites (gray circles) and continuous stations (numbered, white circles). The Río San Miguel basin (~3796 km^2) is delineated above a discharge observation point at El Cajón (black square) based on a 86-m DEM. The subwatershed of the Río San Miguel containing the soil moisture observations used in this study is shown.

Table 1
Data availability from the PSR/CX sensor (number of 800-m pixels) and transect data (number of sampling locations) in the study basin

Date	DOY	PSR/CX pixels	Transect sites
08/03/2004	216	–	15
08/04/2004	217	–	14
08/05/2004	218	154	30
08/06/2004	219	–	15
08/07/2004	220	133	15
08/08/2004	221	152	30
08/09/2004	222	154	15
08/10/2004	223	154	15
08/11/2004	224	–	30
08/12/2004	225	154	14
08/13/2004	226	154	16
08/14/2004	227	154	9

through the region: Río San Miguel (west) and Río Sonora (east), with the former draining into the latter just south of the study area. A discharge observation point at El Cajón was used to delineate the Río San Miguel basin (~3796 km^2) from a 86-m digital elevation model (DEM). Also depicted in Fig. 1b are the locations of the regional stations, each equipped with a rain gauge and a soil moisture sensor, and transect sites visited during the campaign.

We focus our analysis on a ~100 km^2 basin draining into the Río San Miguel. Vegetation types include desert scrub, mesquite forest, subtropical scrub and oak savanna. In the basin, oak savanna is the upper-most community at elevations greater than 1200-m. A large elevation range (800 to 1200-m) along steep slopes is occupied by deciduous subtropical scrublands which leaf-on during rainy periods (Brown, 1994). River valleys are occupied by mesquite trees, while low elevations (<800-m) are composed of mixtures of drought-tolerant trees, shrubs and cacti. Three major soil types are distinguished in the basin. At high elevations (>900-m), soils are coarse-textured Lithosols with limited depth. At intermediate heights (700 to 900-m), soils are medium-textured Eutric Regosols developed over unconsolidated conglomerates. At low altitudes (<700-m) and along streams, soils consist of coarse-textured Eutric Fluvisols on Quaternary alluvium.

2.2. Ground-based and remotely-sensed data sets

We carried out a soil moisture field experiment in the study region in early August 2004 to coincide with the NAM (e.g., Douglas et al., 1993; Sheppard et al., 2002). Thirty sites along the transect were sampled daily from August 3 to 14, 9:00 A.M. to 4:00 P.M., to coincide with aircraft flights (see Table 1 for data availability). Sampling sites along a rural road were selected to represent elevation bands and ecosystems in the basin despite the limited access. A global positioning system (GPS) sensor was used to obtain the coordinates of each site. While sampling was not simultaneous at all sites, an attempt was made to conduct measurements at a similar time each day for each transect location. Morning samples were taken at high altitudes along the transect, while at lower elevations measurements were made later in the day.

At each transect sampling site, volumetric soil moisture (θ_v in %) was sampled at five locations in a ~2-m by ~2-m plot. We used a commercially-available impedance probe (Delta-T Devices Theta probe, ML2x) to infer the soil moisture content over the 0 to 6-cm soil depth. The sensor uses a voltage standing wave method to estimate the relative probe impedance which is related to the dielectric constant of the soil matrix (Cosh et al., 2005). A factory calibration for mineral soils was used to convert the raw voltage readings to volumetric soil moisture and then compared with soil moisture obtained via a gravimetric method. Gravimetric samples were taken daily at two sampling depths (0–3 cm and 3–6 cm) at each transect site. Vivoni et al. (2007) found good agreement in soil moisture estimates from the sensor readings and gravimetric samples.

The field study was complemented with topographic and remotely-sensed soil moisture data. DEMs at three resolutions (29-m, 86-m, 862-m) were obtained from different contour maps (Instituto Nacional de Estadística, Geografía e Informática, 1997, 1998, 2000). Fig. 2 depicts the soil moisture estimates from the Polarimetric Scanning Radiometer (PSR/CX) for three dates, in relation to the basin boundary. Note the progressive regional drying during the period. The PSR/CX is a microwave imaging radiometer with four channels and dual

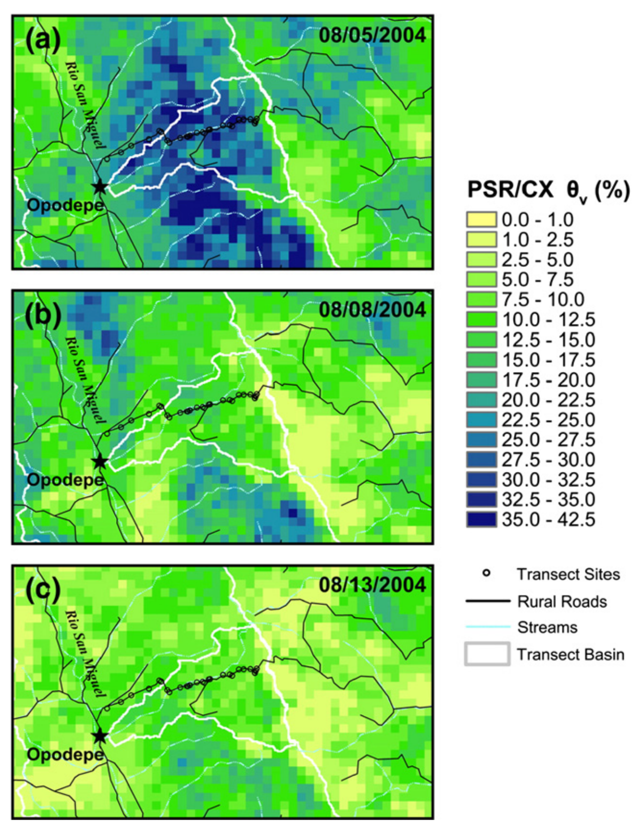

Fig. 2. Evolution of volumetric surface soil moisture (% vol. over 0 to 5 cm) retrieved from the Polarimetric Scanning Radiometer (PSR/CX) using 7.32 H GHz brightness temperature. Each image is sampled to an 800-m resolution and projected to UTM 12N, WGS 1984. The study basin (white polygon) and location of rural roads (black lines) and ephemeral streams (blue lines) are shown. (a) August 5, 2004 (flight time 3:14 to 4:01 P.M.). (b) August 8, 2004 (flight time 9:23 to 10:11 A.M.). (c) August 13, 2004 (flight time 9:37 to 10:24 A.M.).

polarizations in C- and X-band (Jackson et al., 2005). The sensor was flown on a NRL P-3 aircraft at four high-altitude (7300-m), parallel flight lines, with an incidence angle of 55° and swath width of 19-km. The PSR/CX data was processed to obtain a 7.32H GHz brightness temperature and then converted via a retrieval algorithm to an 800-m soil moisture field (see Bindlish et al., 2008-this issue for details). Dense vegetation is accounted for through a canopy layer by using weekly estimates of land cover and vegetation water content from Landsat. Table 1 presents the PSR/CX data availability.

2.3. Analysis techniques

Ground and remotely-sensed soil moisture estimates are characterized by: (1) performing statistical analysis of the spatial and temporal distributions, (2) identifying locations of temporal persistence, (3) assessing the relation between soil moisture statistics and terrain attributes, and (4) comparing soil moisture from arithmetic and hypsometric averaging of ground measurements to the remotely-sensed estimate over the basin.

The statistical analysis consists of characterizing the soil moisture distributions through sample moments and frequency histograms. The spatial mean of the volumetric soil moisture ($\overline{\theta_v^t}$) in the basin for each sampling day is computed as:

$$\overline{\theta_v^t} = \frac{1}{n_t}\sum_{i=1}^{n_t}\theta_{v,i}, \tag{1}$$

where n_t is the number of samples in a given date $t=1, 2,\ldots, N_t$ (total number of dates), and $\theta_{v,i}$ can be either the PSR/CX pixel soil moisture values or the average soil moisture measured in a plot based on five samples. Spatial standard deviation, $\sigma(\theta_v^t)$, and the coefficient of variation (CV_t) of the volumetric soil moisture within the basin are defined as:

$$\sigma(\theta_v^t) = \sqrt{\frac{1}{n_t-1}\sum_{i=1}^{n_t}\left(\theta_{v,i}-\overline{\theta_v^t}\right)^2}, \text{ and} \tag{2}$$

$$\mathrm{CV}_t = \frac{\sigma(\theta_v^t)}{\overline{\theta_v^t}}. \tag{3}$$

The temporal mean of the volumetric soil moisture ($\overline{\theta_v^s}$) at each sampling location over the sampling period is computed as:

$$\overline{\theta_v^s} = \frac{1}{n_s}\sum_{j=1}^{n_s}\theta_{v,j}, \tag{4}$$

where n_s is the number of sampling time periods at a particular site $s=1, 2,\ldots, N_s$ (total number of sites), and $\theta_{v,j}$ can be the PSR/CX pixel soil moisture or the average soil moisture in a plot. Temporal standard deviation, $\sigma(\theta_v^s)$, and the coefficient of variation (CV_s) of the volumetric soil moisture are defined in a similar fashion to Eqs. (2) and (3).

Temporal persistence of soil moisture patterns is assessed through time stability analysis based on the mean relative difference ($\overline{\delta_i}$) (Vachaud et al., 1985) and the root mean square error of the relative difference (RMSE δ_i) (Jacobs et al., 2004). The mean relative difference captures the difference between a location and the spatial mean for all time periods and is evaluated as:

$$\overline{\delta_i} = \frac{1}{N_t}\sum_{t=1}^{N_t}\frac{\theta_{v,i}-\overline{\theta_v^t}}{\overline{\theta_v^t}}, \tag{5}$$

where N_t is the total number of sampling dates and $\theta_{v,i}$ and $\overline{\theta_v^t}$ are defined in Eq. (1). When applied to the PSR/CX data, ($\overline{\delta_i}$) is an 800-m resolution spatial field, whereas for the transect sites, ($\overline{\delta_i}$) is computed at each sampling plot (~4 m^2). Values of ($\overline{\delta_i}$) close to zero indicate that a site captures basin-averaged conditions, while positive (negative) values imply over- (under-) estimation of $\overline{\theta_v^t}$. The variance of the relative difference ($\sigma(\delta_i)^2$) is defined as:

$$\sigma(\delta_i)^2 = \frac{1}{N_t-1}\sum_{t=1}^{N_t}\left(\frac{\theta_{v,i}-\overline{\theta_v^t}}{\overline{\theta_v^t}}-\overline{\delta_i}\right)^2. \tag{6}$$

Small values of $\sigma(\delta_i)^2$ indicate time stable locations where the relative wetness remains similar during the sampling period. The RMSE δ_i is a single metric used to classify time stability with respect to both bias and spread around the bias (Jacobs et al., 2004), and is computed as:

$$\mathrm{RMSE}\delta_i = \left(\overline{\delta_i}^2 + \sigma(\delta_i)^2\right)^{1/2}. \tag{7}$$

Low values of RMSE δ_i indicate time-stable locations that capture basin-averaged conditions.

Soil moisture relations to basin topography are quantified joint frequency distributions. Terrain analysis is used to characterize the topographic field, including its elevation, slope and curvature. Slope and curvature are computed over a 3×3 window using algorithms described in Moore et al. (1991) and implemented in a GIS (ESRI, 1992). The slope represents the change in elevation and captures steepness, while curvature is the change in slope and identifies convex or concave areas. Terrain attributes are related to soil moisture by constructing joint frequency distributions with the 800-m PSR/CX fields in the basin. To construct these, a 29-m DEM is resampled to 800-m to match the PSR/CX spatial resolution and coverage.

Comparisons between ground and remotely-sensed soil moisture estimates are performed at the basin scale through spatial aggregation for each sampling date. A hypsometric aggregation accounting for the area–altitude relation (e.g., Strahler, 1952) is compared to simple arithmetic averaging. The hypsometric method weights the ground data using the fraction of the total basin area in the elevation band encompassing the site of interest. As a result, the method captures the relation between soil moisture and elevation along the transect. Vivoni et al. (in 2007) used the method to assess the temporal variation in hydrometeorological conditions in the basin.

3. Results

In the following, we utilize the ground and remotely-sensed data to assess the spatial and temporal variability of soil moisture in the basin. The reader is referred to Vivoni et al. (2007) for details on the regional rainfall distribution prior to and during the sampling period. We focus here on the statistical analysis, temporal persistence and relations between terrain attributes and soil moisture measurements. Field data and PSR/CX retrievals are compared during the study period, with emphasis placed on three dates having nearly complete spatial coverage.

3.1. Statistical characterization of soil moisture fields

Transect measurements and PSR/CX retrievals provide a unique opportunity to assess the spatiotemporal variability of soil moisture in mountain regions. For example, a relation between mean soil moisture and its spatial variability would be useful information in the NAM region (Gochis et al., 2006). Fig. 3a presents the spatial standard deviation, $\sigma(\theta_v^t)$, as a function of spatial mean soil moisture for ground and remotely-sensed data. For both estimates, the standard deviation increases with mean water content, indicating the soil moisture field becomes more variable for wet conditions. In the semiarid region, absolute spatial variability is lower for drier states. This behavior is consistent with observations in semiarid Spain (Martínez-Fernández & Ceballos, 2003), but differs from studies in more humid areas (e.g., Bell et al., 1980; Famiglietti et al., 1999), where the standard deviation is weakly related to spatial mean moisture content.

Table 2
Linear regressions of the mean soil moisture ($\overline{\theta_v^t}$) with the standard deviation, $\sigma(\theta_v^t)$, and coefficient of variation (CV_t) for the transect sites and PSR/CX retrievals

Estimation method	Slope [−, 1/%]	Intercept [%, −]	R^2 [−]
$\sigma(\theta_v^t)$ vs. $\overline{\theta_v^t}$			
Transect sites	0.51±0.10	−1.04±0.79	0.74
PSR/CX pixels	0.25±0.03	1.21±0.34	0.94
Both estimates	0.27±0.03	0.92±0.30	0.84
CV_t vs. $\overline{\theta_v^t}$			
Transect sites	0.02±0.02	0.24±0.10	0.17
PSR/CX pixels	−0.01±0.00	0.52±0.05	0.64
Both estimates	−0.01±0.00	0.45±0.04	0.18

For each relation, the slope and intercept are presented with estimates of ±1 standard error (SE). The coefficient of determination (R^2) indicates the fraction of variance explained by the regression. Dimensionless parameters indicated with a dash [−].

The relative variability (CV_t in Fig. 3b) decreases with increasing water content for the PSR/CX estimates, while the transect data exhibit an increasing trend. This discrepancy is due to the differences in the range of the mean water contents. The mean soil moisture ranges from 2.6 to 25.3% for PSR/CX pixels and from 5.95 to 11.93% for transect sites. The large range of $\overline{\theta_v^t}$ for the remotely-sensed data results in a decrease in the relative

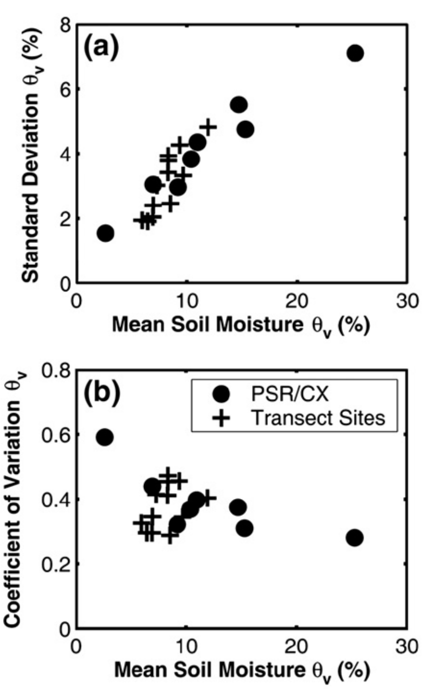

Fig. 3. Statistical characterization of volumetric soil moisture in the study basin. (a) Spatial standard deviation ($\sigma(\theta_v^t)$ in %) and (b) coefficient of variation (CV_t) versus the spatial mean soil moisture ($\overline{\theta_v^t}$ in %) from the PSR/CX sensor (solid circles) and transect site data (crosses). Each symbol represents a separate sampling date. For the PSR/CX, the statistics are obtained for the 800-m products clipped to the basin boundary. For the field measurements, daily transect site averages are used to obtain the statistics via simple arithmetic averaging.

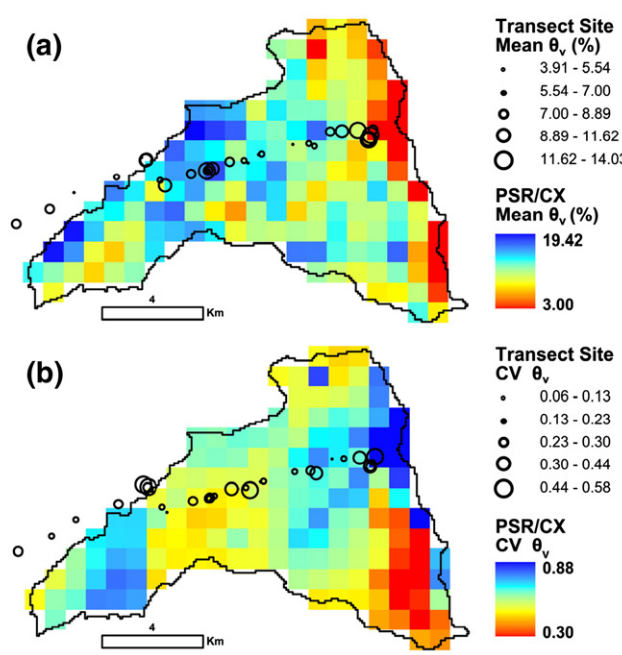

Fig. 4. (a) Temporal mean of the volumetric soil moisture ($\overline{\theta_v^s}$ in %) and (b) coefficient of variation (CV_s) for the PSR/CX pixels (colored pixels) and transect site locations (circles).

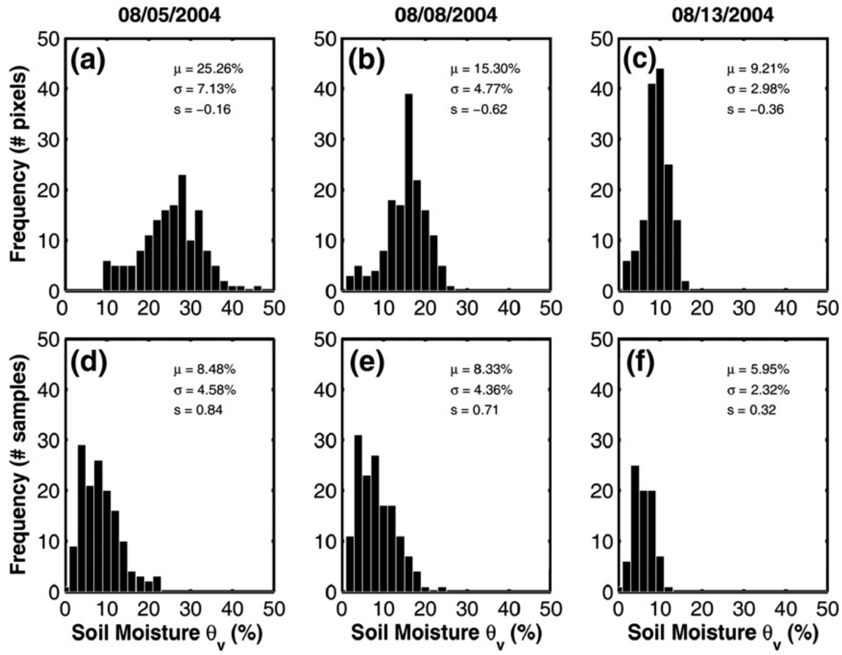

Fig. 5. Frequency distributions of soil moisture (θ_v in %) in the study basin for selected dates. (top row) Frequency distribution of PSR/CX data. (bottom row) Frequency distribution of all daily transect samples. Statistical properties (mean μ (%), standard deviation σ (%), and skewness s) are shown for each distribution (bin width of 2% θ_v used).

variability with higher moisture contents, consistent with Bell et al. (1980), Charpentier and Groffman (1992) and Famiglietti et al. (1999). This behavior is not observed for the transect sites due the limited range in mean soil moisture. Despite this, it is interesting to note that the variation with mean soil moisture for the PSR/CX estimates bound the transect site relations (see Table 2 for linear regression statistics).

Spatial variability of basin soil moisture was assessed by comparing temporal statistics of the ground and remotely-sensed estimates. Temporal mean soil moisture ($\overline{\theta_v^s}$) for the PSR/CX pixel and transect site data is shown in Fig. 4a. At high elevations with oak savanna, the transect sites exhibit high $\overline{\theta_v^s}$, while the PSR/CX pixels depict low water contents. At lower elevations with subtropical scrub, however, the

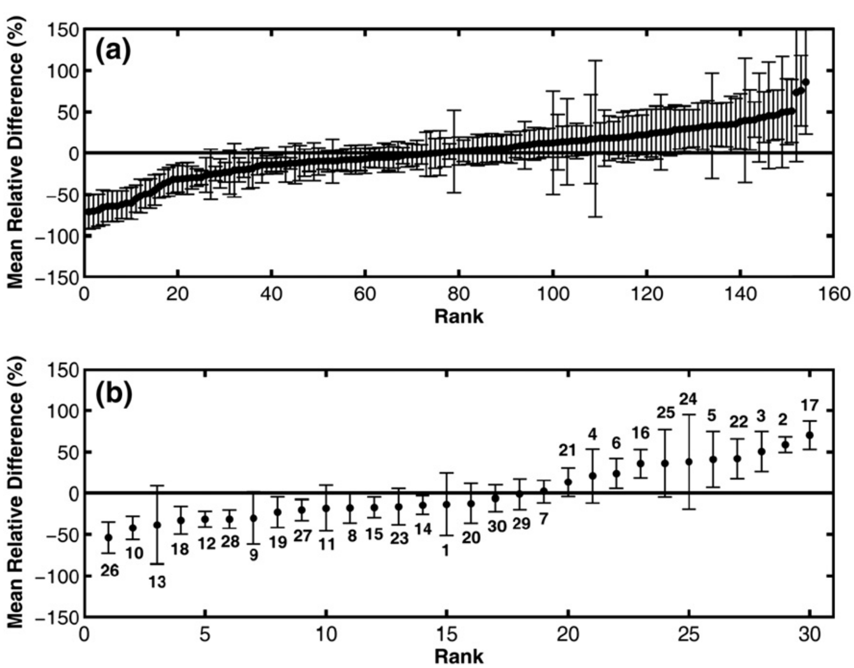

Fig. 6. (a) Ranked mean relative difference ($\overline{\delta_i}$) for all PSR/CX pixels in the basin with ±1 standard deviation of the relative difference, $\sigma(\delta_i)$. (b) Ranked mean relative difference ($\overline{\delta_i}$) for the transect sites with $\pm 1\sigma(\delta_i)$. Both $\overline{\delta_i}$ and $\sigma(\delta_i)$ (dimensionless) are expressed as a percentage (%) by multiplying by 100. Note that the labels in (b) indicate the transect site number.

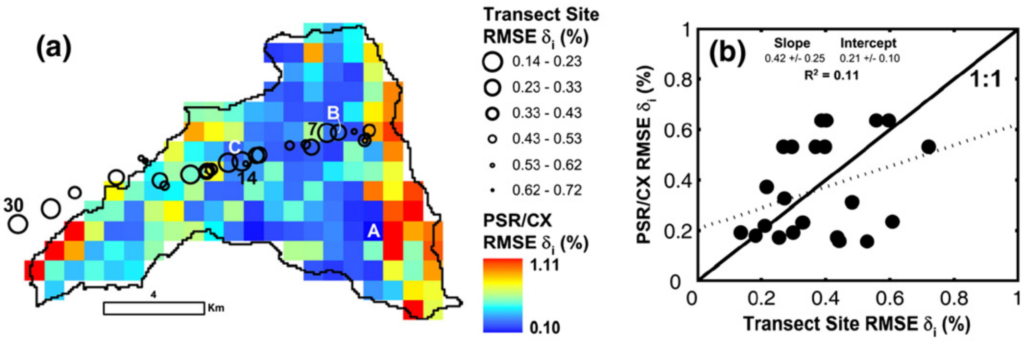

Fig. 7. (a) RMSE δ_i, of the transect sites and PSR/CX soil moisture fields. Larger symbols and bluer colors indicate time-stable locations. (b) Comparison of RMSE δ_i at co-located transect sites and PSR/CX pixels in the study basin (sites 1 to 23) with respect to a 1:1 line (perfect fit). The dashed line represents a linear regression with slope and intercept (±1SE) and R^2 indicated. The standard error of estimation (SEE) is 0.19 and the bias is 4%.

agreement is improved with both estimates revealing wet conditions. CV_s (Fig. 4b) indicates that, despite differences in mean soil moisture, both estimates exhibit similarities in temporal variability. High elevations show large temporal variations (high CV_s), while low elevations are characterized by less variable soil moisture (low CV_s). However, CV_s for PSR/CX estimates are higher than ground data, suggesting the remotely-sensed estimates are less consistent despite similar flight times, potentially due to vegetation changes. In addition, the CV_s field contains sharp transitions between coherent regions, which may be indicative of artifacts in the PSR/CX processing related to vegetation or land cover conditions.

To further characterize the soil moisture estimates, Fig. 5 presents frequency distributions for three sampling dates (August 5, 8 and 13, 2004). The distributions contain all of the PSR/CX pixels in the basin (Fig. 5a–c), as well as all samples (5 in each plot) at the transect sites (Fig. 5d–f). There is a progressive drying in both frequency distributions with corresponding changes in the histogram. The two methods yield significantly different distributions during the early wet period, yet become more similar for drier conditions. As the basin dries, mean soil moisture and standard deviation decrease. Interestingly, the skewness of the PSR/CX estimates are negative, while the transect data have positive skewness. This is an important distinction related to the control exerted by mean soil moisture on the skewness (Famiglietti et al., 1999).

3.2. Temporal persistence of soil moisture patterns

The temporal persistence of soil moisture spatial patterns can help identify how landscape characteristics affect basin hydrology (Jacobs et al., 2004; Mohanty & Skaggs, 2001). While this has been studied in various areas, similar analysis has not been performed in the NAM region. Time stability can also reveal locations in a watershed that represent soil moisture averaged over large scales (Cosh et al., 2004). Ranked mean relative difference ($\bar{\delta_i}$) and the standard deviation of the relative difference are shown in Fig. 6 for the PSR/CX pixel and transect sites. For each estimate, there are several sites that show time stability. Transect sites 7 (at 1122-m, subtropical scrub), 14 (at 868-m, mesquite forest) and 30 (at 669-m, desert scrub) in different elevations and vegetation communities are time-stable locations. In addition, Fig. 6 allows identification of sites that are persistently wetter (high $\bar{\delta_i}$) or drier (low $\bar{\delta_i}$) than basin-averaged conditions.

The RMSE δ_i of the transect sites and PSR/CX estimates are compared in Fig. 7. Good agreement is exhibited in the spatial pattern of the temporal persistence from both methods (Fig. 7a). Time-stable locations that capture the basin-average (low RMSE δ_i) are concentrated at mid elevations, while sites with time-variable conditions (high RMSE δ_i) tend to be located at low and high elevations. The RMSE δ_i from the PSR/CX pixels exhibit high spatial coherency which may be related to elevation or landscape features. For example, regions of high and low RMSE δ_i are similar to the pattern of the subtropical scrub and oak savanna, respectively. This may be due to vegetation impacts on

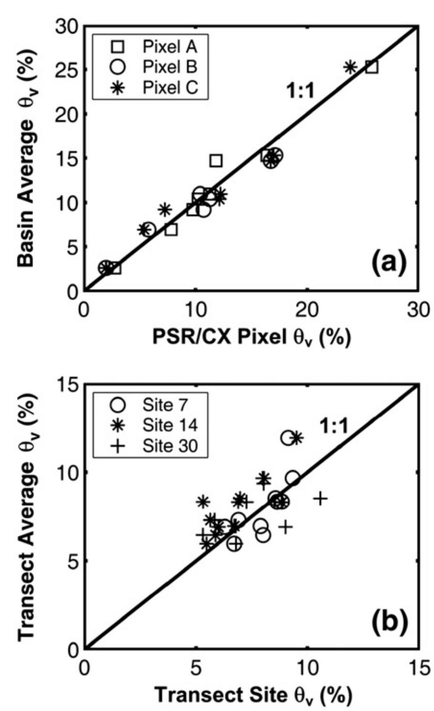

Fig. 8. Comparison of daily soil moisture measurements (θ_v in %) at representative locations and the transect or basin-averaged conditions. (a) Daily PSR/CX soil moisture at locations (A, B, C) versus the basin-averaged soil moisture (all 154 pixels). (b) Daily site average soil moisture (based on five samples) at three sites (7, 14, 30) versus the transect average soil moisture.

Table 3
Linear regressions between representative locations and basin or transect averages

Representative location	RMSE δ_i [−]	Slope [−]	Intercept [−]	R^2 [−]
Pixel A	0.10	0.98±0.07	0.19±1.01	0.97
Pixel B	0.19	0.70±0.04	2.49±0.59	0.98
Pixel C	0.18	0.92±0.09	0.79±1.27	0.94
Three pixels		0.82±0.05	1.65±0.67	0.94
Site 7	0.14	1.24±0.38	−1.94±3.08	0.57
Site 14	0.18	0.95±0.24	1.57±1.66	0.64
Site 30	0.17	0.40±0.24	4.72±1.90	0.25
Three sites		0.67±0.16	2.96±1.21	0.38

RMSE δ_i used to select the representative sites. Slope and intercept of the linear regression include estimates of ±1 SE and R^2.

the PSR/CX retrieval. In Fig. 7b, RMSE δ_i is compared at the transect sites by selecting the nearest PSR/CX pixel. The correspondence in RMSE δ_i indicates that the estimates have similar capabilities in identifying time-stable locations.

Identifying sites that capture basin-averaged soil moisture can help reduce the number of sampling points needed to validate remotely-sensed estimates (Cosh et al., 2004; Grayson & Western, 1998). We selected locations with the lowest RMSE δ_i in the PSR/CX field (pixel A) and transect (site 7), as well as sites with low RMSE δ_i, but present at other elevations (sites 14, 30). For comparison, we found the closest PSR/CX pixels to sites 7 and 14. Fig. 8a compares the PSR/CX pixel soil moisture to the spatial mean based on all pixels. Note the excellent agreement between the pixel estimates and the basin-averaged soil moisture. Similarly, Fig. 8b compares the daily transect soil moisture at sites 7, 14 and 30 to the transect-averaged values. While the regression statistics in Table 3 reveal the correlations are low, it is still possible to estimate transect-averaged conditions fairly well. This indicates that representative locations can capture soil moisture conditions in large footprints even in regions with high topographic variability.

3.3. Terrain controls on soil moisture distribution

Terrain controls on soil moisture distributions have been studied in a variety of locations, typically at small scales (e.g., Crave & Gascuel-Odoux, 1997; Hawley et al., 1983). In the NAM region, the lack of soil moisture observations has inhibited analysis of terrain controls. Based on Grayson et al. (1997), terrain attributes influence soil moisture distributions after rainfall events, while drier conditions resemble soil or vegetation patterns. To determine terrain effects on the PSR/CX estimates, we resampled the 29-m DEM to match the spatial resolution and coverage of the aircraft data. The resampled 800-m DEM retains the slope and curvature characteristics of the 29-m DEM well (not shown), suggesting it captures the topographic features in the basin and can be used for comparison with the PSR/CX soil moisture fields.

Fig. 9 presents joint frequency distributions of terrain attributes and soil moisture statistics from the PSR/CX estimates. The statistics shown are the temporal mean soil moisture ($\overline{\theta}_v^s$), the temporal coefficient of variation (CV_s) and the RMSE δ_i of the relative difference, each compared to the elevation (m), slope (degrees) and curvature (1/100 m^{-1}) fields. Joint frequency distributions indicate the number of PSR/CX pixels that occupy particular values of the terrain attribute and soil moisture statistic. A larger number of pixels mean more frequent occurrences of the combined values. Fig. 9 (top row)

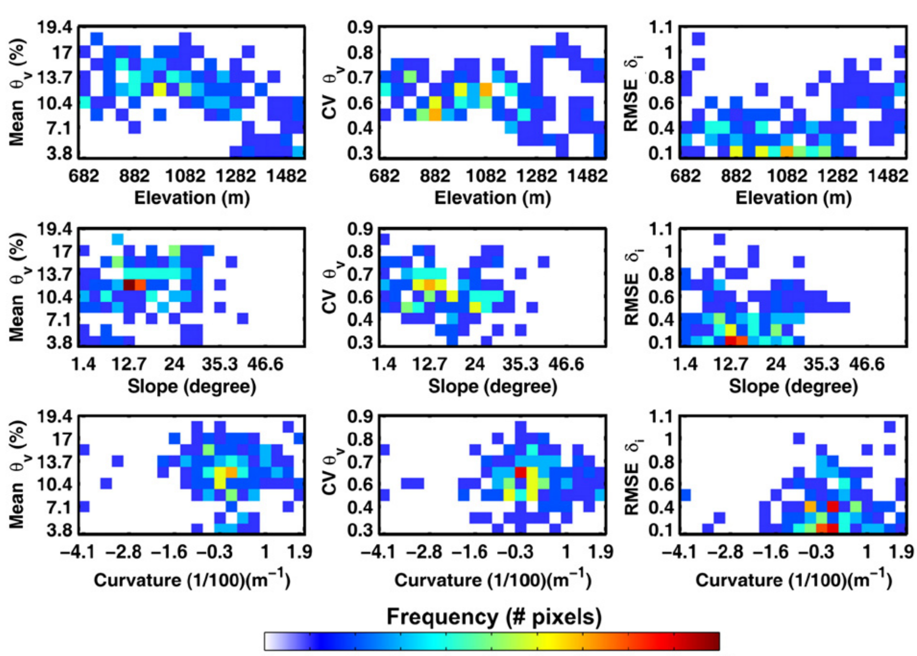

Fig. 9. Joint frequency distributions of terrain attributes derived from a 800-m DEM and soil moisture statistics derived from the 800-m PSR/CX fields. Statistics include temporal mean soil moisture ($\overline{\theta}_v^s$ in %, right column), temporal coefficient of variation (CV_s, middle column) and root mean square error of the relative difference (RMSE δ_i, left column). Terrain attributes are elevation (m, top row), slope (degrees, middle row) and curvature (1/100 m^{-1}, bottom row).

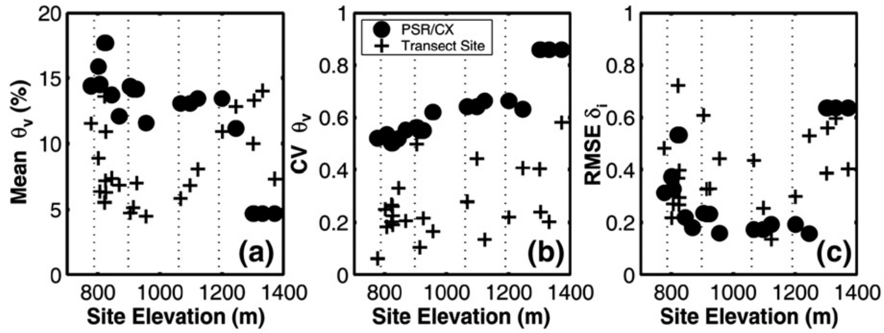

Fig. 10. Elevation variation of the soil moisture statistics from PSR/CX retrievals and transect data. (a) Temporal mean soil moisture ($\overline{\theta_v^s}$ in %). (b) Temporal coefficient of variation (CV_s). (c) Root mean square error of relative difference (RMSE δ_i). Transect sites located inside the basin (sites 1 to 23) are compared to the nearest PSR/CX pixel. The vertical dashed lines represent divisions between physiographic regions along the transect.

highlights the control exerted by elevation on the temporal mean soil moisture and its temporal variability. Mid-elevations in the basin (~800 to ~1100-m) are characterized by high mean soil moisture exhibiting moderate-to-low temporal variability (CV_s) and soil moisture values that are time stable (low RMSE δ_i). At high and low basin elevations (<800-m and >1100-m), the mean soil moisture decreases and the temporal variability increases, with a corresponding decrease in time stability (high RMSE δ_i).

Slope does not appear to have a strong relation with mean soil moisture, although there are many intermediate-slope pixels (~12–15°) with high mean soil moisture (~10–13%). These pixels also have high time-stability (low RMSE δ_i) indicating persistent wet conditions. With respect to curvature, concave pixels (−30 to −90 m^{-1}) have higher mean water contents (~10–15%) as compared to convex pixels (0 to 100 m^{-1}, ~7–12%), implying that terrain convergence affects soil moisture distributions. Furthermore, concave pixels along valley bottoms also have slightly higher time-stability (lower RMSE δ_i). Based on the joint frequency distributions, terrain controls on the PSR/CX soil moisture estimates appear to exist in the basin during the study period. As noted by Vivoni et al. (2007), topographic effects on soil moisture are amplified for the early, wet conditions and reduced during the later, drying phase.

To further explore terrain controls, we compare the PSR/CX and transect data at 23 co-located sites. Temporal mean soil moisture ($\overline{\theta_v^s}$), coefficient of variation (CV_s) and RMSE δ_i are shown in Fig. 10 as a function of elevation. PSR/CX estimates vary with altitude, overestimating soil moisture with respect to ground data at low sites and underestimating water content at high elevations (Fig. 10a). Except in the oak savanna, the overall trends with altitude are consistent in the estimates, with a marked positive bias of ~2–10% in the PSR/CX retrievals. The temporal CV_s increases with elevation at a rate of 0.03–0.06 per 100-m, with more scatter observed in the ground data (Fig. 10b). The PSR/CX estimates consistently show a positive bias of ~0.3 to 0.5 in CV_s with respect to the transect data. Variations of RMSE δ_i with elevation have similar behavior (Fig. 10c), with high time-stability at mid-elevations and low time-stability at low and high altitudes. It is clear from this analysis that soil moisture statistics are influenced by elevation and landscape features and that PSR/CX overestimates soil moisture except at high elevations.

3.4. Hypsometric aggregation of soil moisture

Soil moisture fields averaged over large footprints allow comparisons to retrievals from remote sensors (Cosh et al., 2004; Jackson et al., 2005). Fig. 11 depicts an aggregation method using the basin hypsometry which results in soil moisture averages comparable to remote sensing scales. Five elevation regions derived from a 86-m DEM are used to represent distinct landforms (Mountain, Slope, Footslope, Valley, Lower Valley). Each region is characterized by a fraction of the basin area and an elevation difference. Transect site soil moisture values in an elevation region are arithmetically averaged and then weighted according to the fraction of the total area occupied by the elevation band. To perform the analysis, transect sites outside the basin were assumed as valid representations of similar elevations in the watershed (Vivoni et al., 2007).

To test the value of elevation for aggregating soil moisture, we compare the hypsometric technique to simple arithmetic averaging of all transect sites. Basin-averaged soil moisture is computed for eight sampling dates with simultaneous ground and remote sensing data (Fig. 12). Hypsometric aggregation of the transect data captures features of the averaged PSR/CX data,

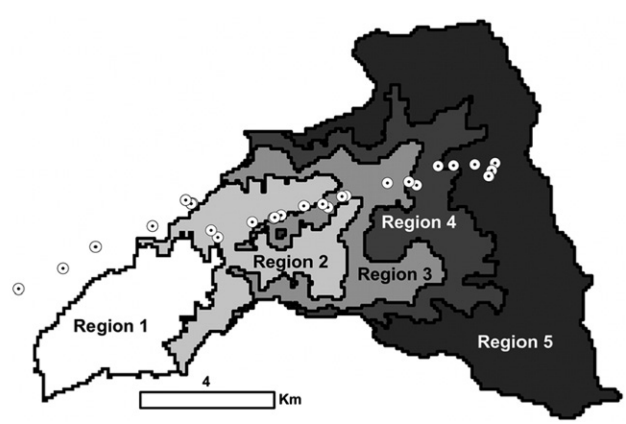

Fig. 11. Distribution of elevation bands or regions based on the 86-m DEM, along with the location of the transect sites (circles). The regions are characterized by the following elevations: Region 1 (Lower Valley, 643 to 797-m), Region 2 (Valley, 797 to 899-m), Region 3 (Footslope, 899 to 980-m), Region 4 (Slope, 980 to 1098-m), and Region 5 (Mountain, 1098 to 1621-m). The upper and lower sites correspond to 1371-m (site 1) and 669-m (site 30), respectively.

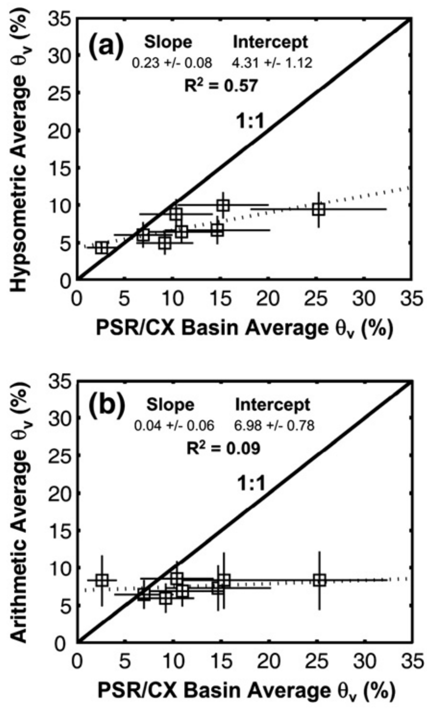

Fig. 12. Comparison of basin-averaged soil moisture ($\overline{\theta_v^t}$ in %) from ground and remotely-sensed estimates. (a) Hypsometric averaging of the transect data based on the 800-m DEM. (b) Arithmetic averaging of the transect measurements. The PSR/CX basin-averaged soil moisture is obtained by arithmetic averaging. Square symbols represent the spatial mean values for each sampling date, while vertical and horizontal bars are the spatial standard deviation ($\sigma(\theta_v^t)$ in %). The dashed line represents a linear regression with slope and intercept (±1SE) and R^2 indicated.

as indicated by the positive slope and high linear correlation, although the standard error of estimation (SEE) is high and bias is present (SEE = 6.97, bias = 41%). In contrast, the arithmetic aggregation has a slightly poorer fit to the averaged PSR/CX estimates (SEE = 7.53, bias = 37%, Fig. 12b). Small improvements obtained through the hypsometric technique are attributed to the fractional area weighting during both wet and dry periods. For example, high elevations with wet conditions are weighted heavily due to the large fractional area, thus increasing basin-averaged soil moisture. Even with this improvement, the correlation of the spatial mean soil moisture from ground-based and remotely-sensed data is fairly weak, due to inherent differences in estimation methods. Overall, the hypsometric method suggests that terrain properties may be useful for aggregating ground data to larger remote sensing scales.

4. Discussion and conclusions

Relatively few ground or remote sensing observations of soil moisture are available in semiarid areas characterized by complex terrain and monsoonal climates. As a result, our current understanding of the spatiotemporal variability of soil moisture in the mountainous NAM region is limited (e.g., Gochis et al., 2006; Higgins et al., 2003; Vivoni et al., 2007). Furthermore, soil moisture can be especially variable in the region due to the seasonal effects of the monsoon and terrain controls on rainfall, vegetation and soil conditions. As shown here, a promising approach for understanding soil moisture patterns during the monsoon season is through the use of field sampling and passive microwave remote sensing. To do so requires accounting for variations in topography, soils and vegetation in the sampling strategy and retrieval algorithms. In particular, difficulties may arise in soil moisture estimation from remote sensing due to terrain effects and dense vegetation in mountain regions. Nevertheless, the spatial information afforded by remote sensing is valuable and thus requires adequate evaluation through comparisons to field data in mountainous regions. This evaluation is challenging due to discrepancies in spatial resolution, sampling period and retrieval method employed by ground and remotely-sensed estimates.

The observational data analysis and interpretations presented in this study identifies the spatiotemporal distribution of soil moisture in mountain landscapes during the North American monsoon. In particular, the field experiment design was focused on assessing the topographic controls on soil moisture through daily sampling over a range of elevations. Intercomparisons to aircraft remote sensing also emphasized the topographic effects in the soil moisture statistics. To our knowledge, this study is the first attempt to evaluate PSR/CX retrievals with respect to ground data over a region of high terrain and vegetation variability using statistical, time-stability and terrain analysis. From the ground and remotely-sensed estimates, we identify the following features of the soil moisture distribution in mountainous areas of northern Sonora, Mexico:

(1) Ground-based and remotely-sensed soil moisture estimates exhibit similar spatial variations with changes in spatial mean water content. Increased spatial variability is observed for wetter basin conditions. Nevertheless, frequency distributions reveal clear differences in soil moisture from the two estimates, in particular for wet periods and high elevations. Temporal variability of the two methods follow similar trends along the transect, with larger day-to-day variations observed in the PSR/CX data.
(2) Temporal persistence estimated from ground-based and remotely-sensed data agree well over the transect and exhibit patterns related to vegetation distribution. Based on the time stability, a set of representative sampling sites and pixels can capture the basin-averaged soil moisture and provide a means for efficient sampling across the topographic transect. Persistent wet or dry locations also exist within the ground and remotely-sensed soil moisture fields.
(3) The spatiotemporal properties of the PSR/CX soil moisture fields are related to terrain attributes. The pixel elevation, slope and curvature play a role in determining the temporal mean soil moisture and variability. Comparison between ground-based and remotely-sensed data along the transect reveal consistent variations with elevation but positive biases in the PSR/CX mean and variability. Comparisons over topographic transects are a useful means to assess remotely-sensed estimates relative to ground observations.

(4) A hypsometric technique may be useful for aggregating ground data to larger remote sensing footprints if appropriate sampling is performed in different elevation bands. The use of topographic information improves comparisons between basin-averaged soil moisture derived from ground-based and remote sensing estimates, as compared to simple arithmetic averaging. Additional tests are required to fully assess the hypsometric aggregation method.

Results of this study are based on soil moisture observations obtained during an intensive observation period in a small domain of the NAM region. Despite the limited temporal extent, the timing of the study included a significant dry down period that enabled comparisons across a range of soil moisture conditions. Ground-based and remotely-sensed estimates over multiple dates allowed the assessment of spatiotemporal soil moisture patterns and the controls exerted by terrain properties. Nevertheless, further analysis is required to understand the regional variation in soil moisture over the larger PSR/CX domain based on comparisons to continuous sensors and regional sampling. In particular, special attention needs to be paid to the effects of seasonal vegetation cover and complex terrain on the PSR/CX soil moisture retrievals. Lessons learned from this study can also be useful for aggregating soil moisture estimates to remote sensing footprints and designing sampling networks to take advantage of the basin hypsometric relation.

Acknowledgements

We would like to acknowledge funding from NASA Terrestrial Hydrology and AMSR-E Validation Programs and the NOAA North American Monsoon Experiment. We would like to thank the SMEX04 participants who conducted the field sampling and aircraft remote sensing. We also thank three anonymous reviewers whose comments helped improve the manuscript.

References

Bell, K. R., Blanchard, B. J., Schmugge, T. J., & Witczak, M. W. (1980). Analysis of surface moisture variations within large-field sites. *Water Resources Research*, *16*(4), 797−810.

Bindlish, R., Jackson, T. J., Gasiewski, A., Stankov, B., Cosh, M. H., Mladenova, I., et al. (2008). PSR based soil moisture estimates in high vegetation and topographic domain. *Remote Sensing of Environment*, *112*, 480−492 (this issue). doi:10.1016/j.rse.2007.01.024.

Brown, D. E. (1994). *Biotic communities southwestern United States and northwestern Mexico.* Salt Lake City, UT: University of Utah Press 342 pp.

Charpentier, M. A., & Groffman, P. M. (1992). Soil moisture variability within remote sensing pixels. *Journal of Geophysical Research*, *97*(D17), 18,987−18,995.

Comisión Nacional del Agua (2002). *Determinación de la disponibilidad de agua en el acuífero Río Sonora, Estado Sonora.* 42 pp.

Cosh, M. H., Jackson, T. J., Bindlish, R., Famiglietti, J. S., & Ryu, D. (2005). Calibration of an impedance probe for estimation of surface soil water content over large regions. *Journal of Hydrology*, *311*, 49−58.

Cosh, M. H., Jackson, T. J., Bindlish, R., & Prueger, J. H. (2004). Watershed scale temporal and spatial stability of soil moisture and its role in validating satellite estimates. *Remote Sensing of Environment*, *92*, 427−435.

Crave, A., & Gascuel-Odoux, C. (1997). The influence of topography on time and space distribution of soil surface water content. *Hydrological Processes*, *11*, 203−210.

Douglas, M. W., Maddox, R. A., Howard, K., & Reyes, S. (1993). The Mexican monsoon. *Journal of Climate*, *6*, 1665−1677.

Eltahir, E. A. B. (1998). A soil moisture rainfall feedback mechanism 1. Theory and observations. *Water Resources Research*, *34*(4), 765−776.

Entekhabi, D. (1995). Recent advances in land–atmosphere interaction research. *Reviews of Geophysics*, *33*(S1), 995−1004.

ESRI, Environmental Systems Research Institute (1992). *Understanding GIS: The ArcInfo method.* Redlands, CA: ESRI Press.

Famiglietti, J. S., Devereaux, J. A., Laymon, C. A., Tsegaye, T., Houser, P. R., Jackson, T. J., et al. (1999). Ground-based investigation of soil moisture variability within remote sensing footprints during the Southern Great Plains 1997 (SGP97) Hydrology Experiment. *Water Resources Research*, *35*(6), 1839−1851.

Famiglietti, J. S., Rudnicki, J. W., & Rodell, M. (1998). Variability in surface moisture content along a hillslope transect: Rattlesnake Hill, Texas. *Journal of Hydrology*, *210*(1–4), 259−281.

Gochis, D. J., Brito-Castillo, L., & Shuttleworth, W. J. (2006). Hydroclimatology of the North American monsoon region in northwest Mexico. *Journal of Hydrology*, *316*, 53−70.

Gómez-Plaza, A., Alvarez-Rogel, J., Albaladejo, J., & Castillo, V. M. (2000). Spatial patterns and temporal stability of soil moisture across a range of scales in a semi-arid environment. *Hydrological Processes*, *14*, 1261−1277.

Grayson, R. B., & Western, A. W. (1998). Towards aerial estimation of soil water content from point measurements: time and space stability of mean response. *Journal of Hydrology*, *207*, 68−82.

Grayson, R. B., Western, A. W., Chiew, F. H. S., & Bloschl, G. (1997). Preferred states in spatial soil moisture patterns: Local and nonlocal controls. *Water Resources Research*, *33*(12), 2897−2908.

Hawley, M. E., Jackson, T. J., & McCuen, R. H. (1983). Surface soil moisture variation on small agricultural watersheds. *Journal of Hydrology*, *62*, 179−200.

Higgins, R. W., Douglas, A., Hahmann, A., Berbery, E. H., Gutzler, D., Shuttleworth, J., et al. (2003). Progress in Pan American CLIVAR Research: North American Monsoon System. *Atmósfera*, *16*, 29−65.

Houser, P. R., Goodrich, D. C., & Syed, K. (2000). Runoff, precipitation and soil moisture at Walnut Gulch. In R. Grayson, & G. Bloschl (Eds.), *Spatial patterns in catchment hydrology: Observations and modelling* (pp. 125−157). Cambridge, UK: Cambridge University Press.

Instituto Nacional de Estadística, Geografía e Informática. (1997). Modelos Digitales de Elevación 1:1,000,000.

Instituto Nacional de Estadística, Geografía e Informática. (1998). Modelos Digitales de Elevación 1:250,000.

Instituto Nacional de Estadística, Geografía e Informática. (2000). Modelos Digitales de Elevación 1:50,000.

Jackson, T. J., Bindlish, R., Gasiewski, A. J., Stankov, B., Klein, M., Njoku, E. G., et al. (2005). Polarimetric scanning radiometer C- and X-band microwave observations during SMEX03. *IEEE Transactions on Geoscience and Remote Sensing*, *43*(11), 2418−2430.

Jacobs, J. M., Mohanty, B. P., Hsu, E. -C., & Miller, D. (2004). SMEX02: Field scale variability, time stability and similarity of soil moisture. *Remote Sensing of Environment*, *92*, 436−446.

Kim, G., & Barros, A. P. (2002). Space-time characterization of soil moisture from passive microwave remotely sensed imagery and ancillary data. *Remote Sensing of Environment*, *81*, 393−403.

Martínez-Fernández, J., & Ceballos, A. (2003). Temporal stability of soil moisture in a large-field experiment in Spain. *Soil Science Society of America Journal*, *67*(6), 1647−1656.

Martínez-Fernández, J., & Ceballos, A. (2005). Mean soil moisture estimation using temporal stability analysis. *Journal of Hydrology*, *312*, 28−38.

Mohanty, B. P., & Skaggs, T. H. (2001). Spatio-temporal evolution and time-stable characteristics of soil moisture within remote sensing footprints with varying soil, slope and vegetation. *Advances in Water Resources*, *24*, 1051−1067.

Mohanty, B. P., Skaggs, T. H., & Famiglietti, J. S. (2000). Analysis and mapping of field-scale soil moisture variability using high-resolution, ground-based data during the Southern Great Plains 1997 (SGP97) Hydrology Experiment. *Water Resources Research*, *36*(4), 1023−1031.

Moore, I. D., Grayson, R. B., & Landson, A. R. (1991). Digital terrain modeling: A review of hydrological, geomorphologic and biological applications. *Hydrological Processes*, *5*, 3−30.

Sheppard, P. R., Comrie, A. C., Packin, G. D., Angersbach, K., & Hughes, M. K. (2002). The climate of the US Southwest. *Climate Research*, *21*, 219−238.

Strahler, A. N. (1952). Hypsometric (area-altitude) analysis of erosional topography. *Bulletin Geological Society of America*, *63*, 1117−1142.

Vachaud, G., Passerat De Silans, A., Balabanis, P., & Vauclin, M. (1985). Temporal stability of spatially measured soil water probability density function. *Journal of the Soil Society of America*, *49*, 822−828.

Vivoni, E. R., Gutiérrez-Jurado, H. A., Aragón, C., Méndez-Barroso, L. A., Rinehart, A. J., & Wyckoff, R. L. (2007). Variation of hydrometeorological conditions along a topographic transect in northwestern Mexico during the North American Monsoon. *Journal of Climate*, *20*(19), 1792−1809.

Zhu, C., Lettenmaier, D. P., & Cavazos, T. (2005). Role of antecedent land surface conditions on North American monsoon rainfall variability. *Journal of Climate*, *18*, 3104−3121.